Safety, Reliability, Risk and Life-Cycle Performance of Structures & Infrastructures – Deodatis, Ellingwood & Frangopol (Eds)
© 2013 Taylor & Francis Group, London, ISBN 978-1-138-00086-5

Tsunami damage assessment of buildings in Chiba Prefecture, Japan using fragility function developed after the 2011 Tohoku-Oki Earthquake

Yoshihisa Maruyama, Ken Kitamura & Fumio Yamazaki
Department of Urban Environment Systems, Chiba University, Chiba, Japan

ABSTRACT: Tsunami fragility functions were developed to assess tsunami-related damage to buildings. The fragility functions were expressed with respect to inundation depth, current velocity, and hydrodynamic force in order to predict damage ratios of buildings. The fragility functions were constructed using numerical simulation results of tsunami propagation and a building damage dataset compiled by Asahi City after the 2011 off the Pacific coast of Tohoku Earthquake and tsunami. Asahi City, Chiba Prefecture, suffered serious damage after this earthquake. Employing the fragility function with respect to inundation depth, the numbers of damaged buildings in Chiba Prefecture were estimated assuming the occurrence of two historical earthquakes.

1 INTRODUCTION

The 2011 off the Pacific coast of Tohoku (Tohoku-oki) Earthquake that occurred on 11 March 2011 triggered an extremely large tsunami. The run-up reached a maximum height of 40.4 m in the Tohoku district (The 2011 Tohoku Earthquake Tsunami Joint Survey Group, 2011). The Japanese National Police Agency (2013) confirmed more than 15,000 dead and 2,600 missing people. According to the Cabinet Office, Government of Japan (2011), 92.4% of the fatalities in the Iwate, Miyagi, and Fukushima prefectures resulted from drowning.

The tsunami also affected Chiba Prefecture, which is located farther from the earthquake source region than the more severely affected areas in the Iwate, Miyagi, and Fukushima prefectures. With 13 fatalities in Asahi City and two people still missing, the eastern part of the prefecture was the most affected. In Asahi City, 336 housing units collapsed as a result of the event (Asahi City, 2011). These buildings were mainly damaged by the tsunami and liquefaction.

Structural performance under tsunami loading has been investigated by various research teams following earlier events (Bertero *et al.*, 1985; Saatcioglu, 2006; Ruangrassamee *et al.*, 2006). Shuto (1993) proposed the tsunami intensity scale based on empirical data from historical tsunamis in Japan to predict structural damage. According to these results, wooden houses are completely destroyed when the tsunami height is greater than 2 m and partially damaged when the tsunami height is 1–2 m. Koshimura *et al.* (2009) proposed the tsunami fragility function as a new measure for estimating tsunami damage. Tsunami fragility is defined as the probability of structural damage based on the hydrodynamic features of tsunami inundation flow, such as inundation depth, current velocity, and hydrodynamic force. Suppasri *et al.* (2012) surveyed damage to buildings in the Miyagi Prefecture after the 2011 Tohoku-oki earthquake and constructed a fragility curve for wooden houses.

In this study, the damage ratio of buildings in Asahi City is evaluated with respect to hydrodynamic features of tsunami inundation flow obtained by numerical simulation. The damage dataset compiled by the Asahi City Government is employed for the evaluation. Fragility functions were constructed based on the relationship between the damage ratio and the hydrodynamic features. Lastly, the number of damaged buildings in Chiba Prefecture is predicted assuming the occurrence of two different historical earthquakes.

2 NUMERICAL SIMULATION OF TSUNAMI PROPAGATION

Numerical simulation of tsunami propagation was performed to estimate the tsunami-inundated areas in Asahi City, Chiba Prefecture after the 2011 Tohoku-oki earthquake. The location of Asahi City is illustrated in Fig. 1. The seismic fault model developed by Fujii *et al.* (2011) was employed to estimate the vertical displacement of the seabed. Figure 1(a, b) shows the fault model of Fujii *et al.* (2011) and the vertical displacement estimated by Okada's method (Okada, 1985). Assuming that the water layer is incompressible, the estimated vertical displacement of the seabed was regarded as the initial profile of the tsunami.

Various methodologies have been employed to simulate tsunami propagation (Ohmachi *et al.*, 2001; Furumura and Saito, 2009; Liu *et al.*, 2008). In this study, we used TUNAMI code (Imamura, 1995) to model the tsunami propagation and resulting coastal

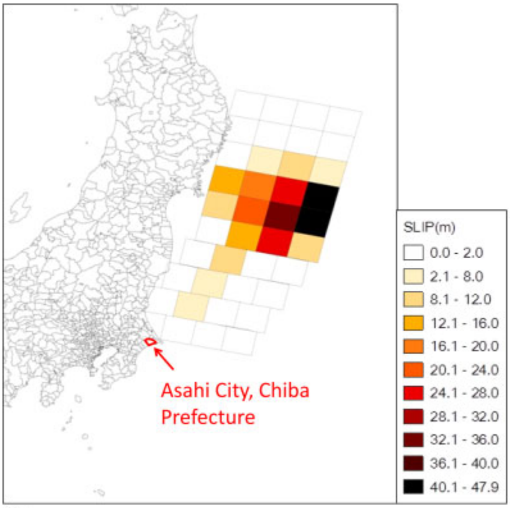

(a)

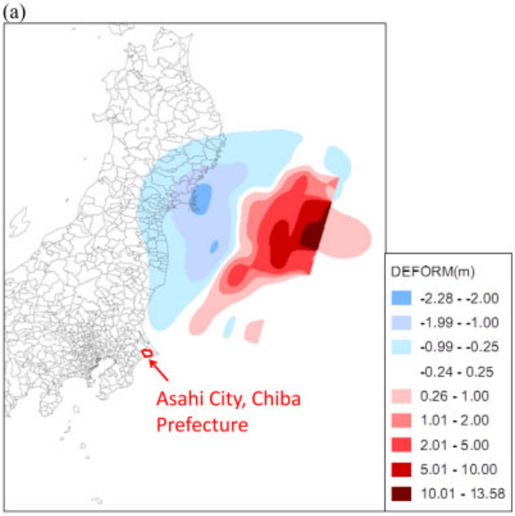

(b)

Figure 1. (a) Fault model developed by Fujii et al. (2011) and (b) vertical displacement of seabed as estimated by Okada's method (1985).

inundation. The model employs a set of nonlinear shallow water equations in which bottom friction terms are discretized by a leap-frog finite difference scheme. This model is widely used for simulating tsunami propagation and inundation on dry land (Koshimura *et al.*, 2006). Based on the shallow water theory, the continuity equation can be expressed as

$$\frac{\partial \eta}{\partial t} + \frac{\partial M}{\partial x} + \frac{\partial N}{\partial y} = 0 \qquad (1)$$

where M and N are the discharge fluxes in the x and y directions, respectively and η is the vertical displacement of the water surface above the still-water level. The equations of motion are written as

$$\frac{\partial M}{\partial t} + \frac{\partial}{\partial x}\left(\frac{M^2}{D}\right) + \frac{\partial}{\partial y}\left(\frac{MN}{D}\right) = -gD\frac{\partial \eta}{\partial x} - \frac{gn^2}{D^{7/3}} M\sqrt{M^2+N^2} \qquad (2)$$

(a)

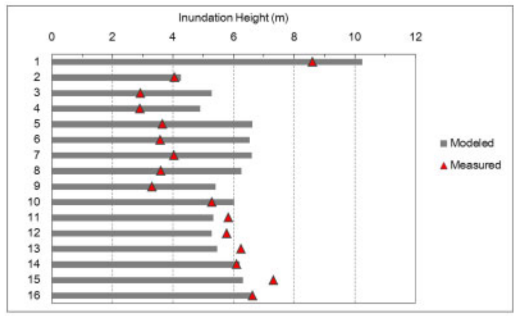

(b)

Figure 2. (a) Locations of measurement points of the tsunami inundation heights from the 2011 Tohoku Earthquake Tsunami Joint Survey Group, and (b) comparison between the measured tsunami inundation heights and those estimated by numerical simulation in Asahi City, Chiba Prefecture.

$$\frac{\partial N}{\partial t} + \frac{\partial}{\partial x}\left(\frac{MN}{D}\right) + \frac{\partial}{\partial y}\left(\frac{N^2}{D}\right) = -gD\frac{\partial \eta}{\partial y} - \frac{gn^2}{D^{7/3}} N\sqrt{M^2+N^2} \qquad (3)$$

where D is the summation of η and the still-water depth h and n is Manning's roughness coefficient.

In the numerical simulation, the target region was divided into five sub-regions having grid lengths of 1350, 450, 150, 50, and 16.7 m. The sub-regions characterized by coarser grids were in the deep sea, and those with finer grids were closer to the shore (Shuto, 1991). h for each grid cell was assigned using bathymetry data collected by the Japan Coast Guard. Land elevations determined by the Geospatial Information Authority of Japan (GSI) were also considered for estimating inundated areas. Manning's roughness coefficients were assigned according to land use classification, as shown in Table 1 (Kotani *et al.*, 1998). We assumed that tsunami propagation occurred for three hours after the earthquake. The time step selected for the numerical simulation was 0.15 s.

The result of the numerical simulation was compared with the findings of tsunami surveys conducted by the 2011 Tohoku Earthquake Tsunami Joint Survey Group (2011). Figure 2 shows a comparison of tsunami inundation heights estimated by the numerical simulation with those measured in the eastern part of Asahi City. The locations of the measurement points of the coastal tsunami inundation heights compiled by the

Table 1. Definition of Manning's roughness coefficient in this study.

Land use	Manning's roughness coefficient ($m^{-1/3}s$)
Residential district	0.040
Agricultural land	0.020
Forest land	0.030
Body of water	0.025
Others	0.025

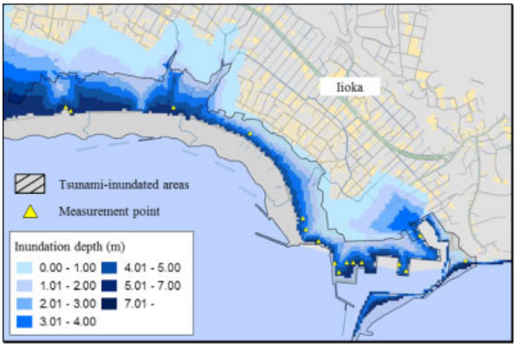

Figure 3. Comparison between inundation depths estimated by numerical simulation and the tsunami-inundated areas identified in Kitamura et al. (2012).

group are also illustrated in Fig. 2. The survey group defined inundation height as the elevation of the water level with reference to sea level (Tokyo Peil: T.P.). According to the comparison, the estimated inundation heights show good agreement with the observations, especially in the residential areas (labeled as 10–16).

Figure 3 shows a comparison of the tsunami inundation depths obtained by the numerical simulation with the tsunami-inundated areas identified in our previous study (Kitamura *et al.*, 2012). Our focus is on the Iioka district, the eastern part of Asahi City, where the inundated areas were verified through different sources. The simulated distribution of tsunami-inundated areas and the distribution identified by our previous study show similar trends, especially in the Iioka district where serious damage to buildings was observed after the tsunami.

3 DEVELOPMENT OF FRAGILITY FUNCTIONS FOR BUILDINGS

This study attempts to evaluate the relationships between the damage ratio of buildings and the hydrodynamic features of tsunami inundation flow in Asahi City, Chiba Prefecture. To achieve this objective, the dataset of damaged buildings compiled by the Asahi City Government was employed. The locations and damage levels of buildings can be identified from the dataset. Four damage levels are defined in the dataset: totally collapsed, heavily half-collapsed, half-collapsed and partially collapsed. Table 2 shows the definitions of the damage levels compiled by the Cabinet Office of the Japanese Government. In this study, the ratio of the number of totally collapsed and heavily half-collapsed buildings to the number of residential buildings is considered as the damage ratio of buildings. We obtained the damage ratios only in the Iioka district, where 178 totally collapsed and 157 heavily half-collapsed buildings were found after the 2011 Tohoku-oki earthquake.

Table 2. Definition of damage levels of buildings.

Damage level	Damage situation
Totally collapsed	Buildings were completely washed away or inundated above the ceiling of the first floor.
Heavily half-collapsed	Buildings were inundated approximately 1 m above floor level.
Half-collapsed	Buildings were inundated just above floor level.
Partially collapsed	Buildings were inundated below floor level.

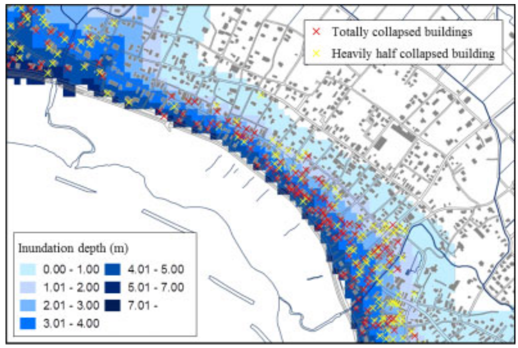

Figure 4. Distribution of damaged buildings according to estimated tsunami-inundation depths in the Iioka District, Asahi City, Chiba Prefecture.

Figure 4 shows the distribution of damaged buildings according to the estimated tsunami-inundation depths in the Iioka district. The building inventory compiled by Zenrin, a Japanese map publisher, in 2009 was employed to identify residential buildings in the Iioka district. The damage ratios of buildings were illustrated with respect to the inundation depths, current velocities, and hydrodynamic forces. The hydrodynamic forces are expressed as

$$F = \frac{1}{2} C_D \rho v^2 d \tag{4}$$

where C_D is the drag coefficient, ρ is the water density, v is the current velocity, and d is the inundation depth. For simplicity, C_D was assumed to be 1.0 (Koshimura *et al.*, 2009). Figure 5 shows the relationships of damage ratio of buildings against inundation depth, current

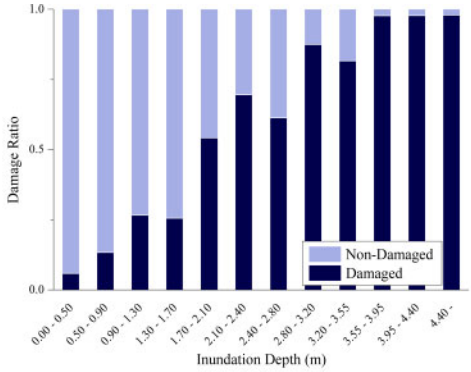

(a)

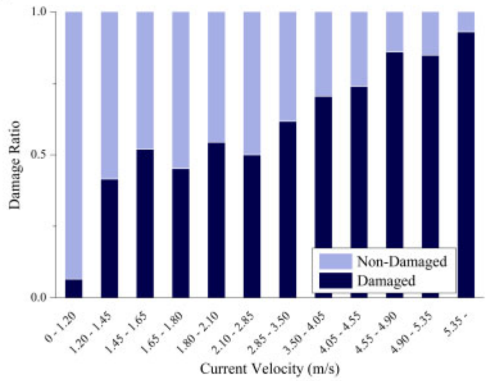

(b)

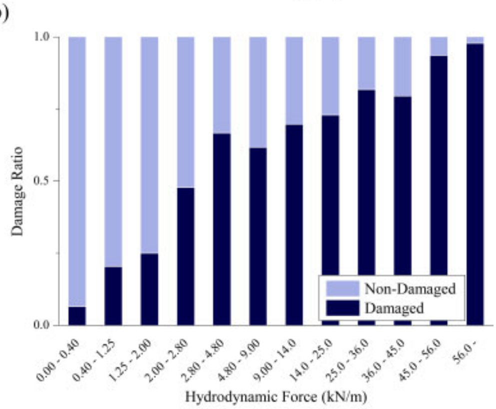

(c)

Figure 5. Damage ratios of buildings in the Iioka District, Asahi City, Chiba Prefecture with respect to (a) inundation depth, (b) current velocity, and (c) hydrodynamic force.

velocity, and hydrodynamic force. As the values of the hydrodynamic features increases, the damage ratio of the buildings also increases. The damage ratio exceeds 50% when the inundation depth is in the range of 1.7–2.1 m and when the current velocity is in the range of 1.8–2.1 m/s.

The damage ratio of buildings, P, is assumed to be the following:

$$P = \Phi((\ln x - \lambda)/\zeta) \tag{5}$$

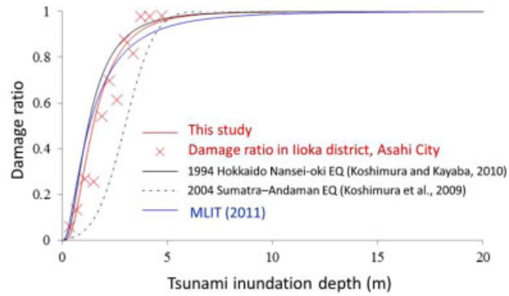

(a)

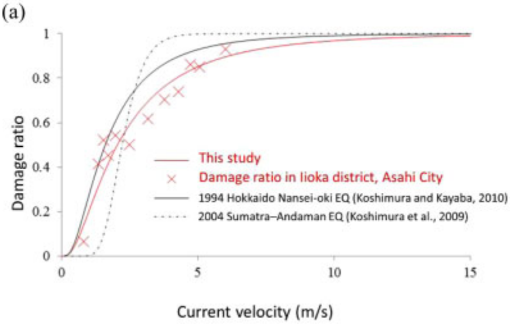

(b)

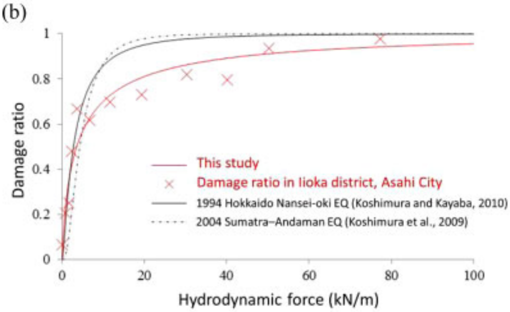

(c)

Figure 6. Fragility functions developed by this study and those estimated after the previous events with respect to (a) inundation depth, (b) current velocity, and (c) hydrodynamic force.

Table 3. Parameters of the fragility functions developed by this study.

Hydrodynamic features	λ	ζ
Inundation depth	0.392	0.675
Current velocity	0.720	0.855
Hydrodynamic force	1.281	1.950

where $\Phi(\cdot)$ is the cumulative distribution function of the standard normal distribution and x is the tsunami inundation depth, current velocity, or hydrodynamic force. λ and ζ are the mean and standard deviation of $\ln x$, which were determined by the least-squares method on lognormal probability paper.

Figure 6 shows the fragility functions for buildings developed in this study. The parameters are listed in Table 3. The fragility functions developed after the 1994 Hokkaido Nansei-oki and 2004 Sumatra-Andaman earthquakes (Koshimura and Kayaba, 2010; Koshimura *et al.*, 2009) are also illustrated in the figure. In these studies, pre- and post-event satellite and aerial images were employed to perform visual damage inspections. The buildings were classified as "survived" or "destroyed" by detecting whether or not their roofs remained and the fraction of "destroyed" buildings was used as the damage ratio. The Ministry of Land, Infrastructure, Transport, and Tourism (MLIT) published the results of a survey after the 2011 Tohoku-oki earthquake. The damage ratios of buildings in the entire region affected by the tsunami are compiled with respect to the inundation depth in their report (MLIT, 2011). A fragility curve was also constructed from this dataset, and this curve is illustrated in Fig. 6(a) for comparison. According to Fig. 6, the fragility function with respect to inundation depth developed by this study gives similar damage ratios as that of the 1994 Hokkaido Nansei-oki earthquake. Although the fragility function of this study is constructed based on the building damage dataset of a municipality, the function shows trends very similar to those of the fragility function based on the damage ratio of buildings in the entire tsunami-affected region compiled by MLIT. The fragility functions with respect to current velocity and hydrodynamic force show smaller damage ratios than those developed after the previous events. These differences are a result of the accuracy of estimation of current velocity in the numerical simulation. As shown in Fig. 2, the inundation depths obtained by numerical simulation were compared with the surveyed data, and the accuracy of the simulated depths was discussed. However, the accuracy of the current velocities has not yet been investigated. This event provided an opportunity to analyze tsunami flow conditions using videos and field evidence (EERI, 2011), and accuracy of current velocity will be realized by employing the videos.

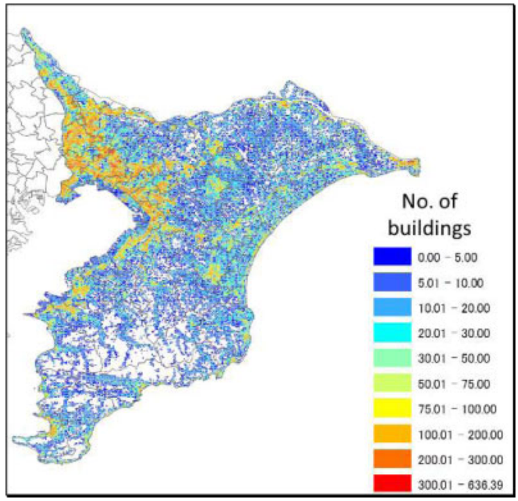

Figure 7. Number of buildings in Chiba Prefecture, Japan (compiled in 2008).

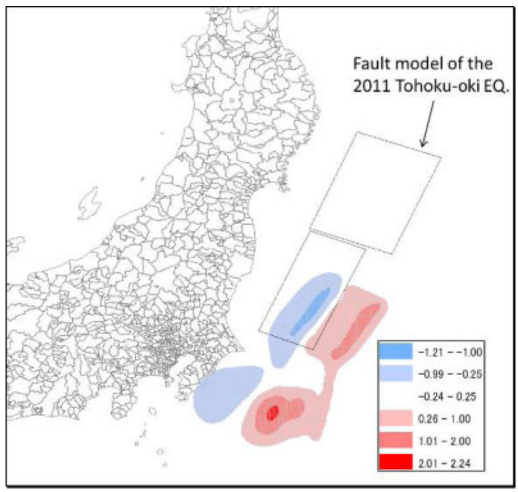

Figure 8. Vertical displacement of seabed assuming the 1677 Empo Boso-oki earthquake and the location of the fault model of the 2011 Tohoku-oki earthquake (GSI, 2011).

4 APPLICATION OF THE TSUNAMI FRAGILITY FUNCTION FOR DAMAGE ASSESSMENT OF BUILDINGS

The fragility function developed by this study is now applied to post-tsunami damage assessment. Based on the findings of the previous section, we employ the fragility curve with respect to inundation depth shown in Fig. 6(a). The damage to buildings in Chiba Prefecture, Japan is estimated assuming the occurrence of historical earthquakes that have struck Chiba Prefecture. Inventory data of buildings compiled by the Chiba Prefectural Government in 2008 for performing loss estimation against scenario earthquakes is used in this study. Figure 7 shows the distribution of the number of buildings, which is represented in 250 m × 250 m grid cells.

Two historical earthquakes were considered in order to assess damage to buildings in Chiba Prefecture. The Empo Boso-oki earthquake occurred in 1677 and generated a large tsunami that struck the Pacific coast of Chiba Prefecture. A tsunami height of 3–8 m was estimated by Takeuchi *et al.* (2007). Figure 8 shows the distribution of seabed vertical displacement, which was used as the initial profile of the tsunami, estimated by Okada's method (Okada, 1985). The fault model developed by Chiba Prefecture was employed to estimate the vertical displacement. The fault model for the 2011 Tohoku-oki earthquake developed by GSI (2011) is also represented in the figure for comparison. The location of the estimated rupture area of the 1677 Empo Boso-oki earthquake is approximately 130 km south of the edge of the fault model for the 2011 event.

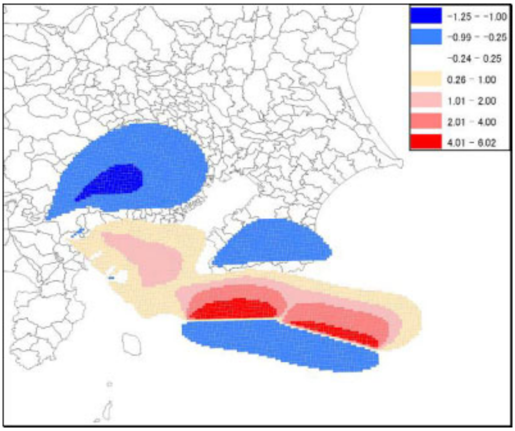

Figure 9. Vertical displacement of seabed assuming the 1703 Genroku Kanto earthquake.

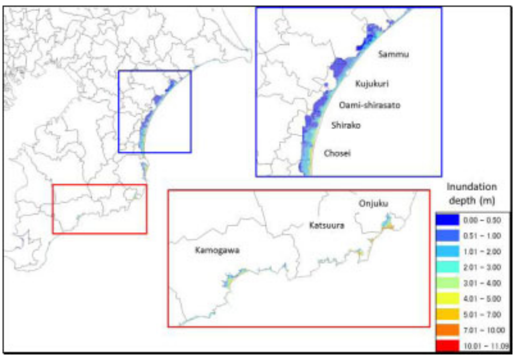

Figure 10. Distribution of estimated inundation depth as-suming the 1677 Empo Boso-oki earthquake.

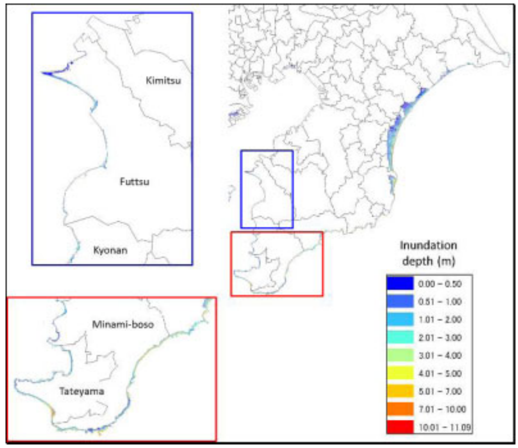

Figure 11. Distribution of estimated inundation depth assuming the 1703 Genroku Kanto earthquake.

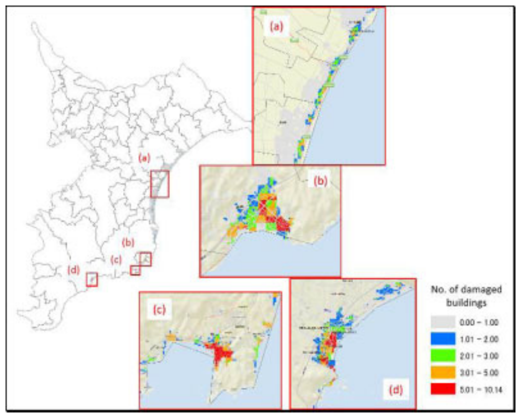

Figure 12. Estimated number of damaged buildings in Chiba Prefecture assuming the 1677 Empo Boso-oki earth-quake.

The other historical earthquake is the 1703 Genroku Kanto earthquake. This event occurred in the south Kanto region, and the tsunami height in the eastern part of Chiba Prefecture was estimated to be 6–11 m (Namegaya *et al.*, 2011). Figure 9 shows the vertical displacement of the seabed assuming the fault model developed by Namegaya *et al.* (2011). The latest earth-quake in the Sagami trough, which had a magnitude of 7.9, occurred in 1923, and the two segments are con-sidered to have high slips. In the 1703 event, another slip occurred at the segment east of the Boso peninsula, resulting in a magnitude of 8.2 (Stein *et al.*, 2006).

Figures 10 and 11 show estimated inundation depth after the two historical earthquakes. The Pacific coast of Chiba Prefecture would be affected by tsunami with an average inundation depth of approximately 5–8 m in both cases. Assuming the occurrence of the 1677 Empo Boso-oki earthquake, tsunami-inundated areas would be spread widely near Kujukuri. Although the inundated areas in Onjuku and Katsuura are nar-row, the maximum inundation depth is estimated to be approximately 10 m (Fig. 10). Severely inundated areas do not occur along Tokyo Bay. For the case of the 1703 Genroku Kanto earthquake, severe inundation occurs in the southern part of the prefecture and also in the eastern part. The maximum inundation depth of 5–8 m occurs in the cities of Tateyama and Minami-Boso. The tsunami progressed northward in Tokyo Bay and reached Cape Futtsu. An inundation depth of 2–3 m is predicted in Futtsu city.

Based on these results, the number of damaged buildings was estimated by employing the fragility function developed by this study. Figures 12 and 13 show the number of damaged buildings in 250 × 250 m grid cells after the two historical earthquakes. The dis-tributions of damaged buildings along the Pacific coast of Chiba Prefecture are similar for both cases. The damaged buildings are concentrated in Kujukuri, Kas-tuura, Kamogawa, and Onjuku. In the case of the 1703 Genroku Kanto earthquake, damage to buildings also occurs along Tokyo Bay, western part of the prefecture (Fig. 13). According to the figures, more than 20,000 buildings could be affected by tsunami in both cases. These results may be helpful for making decisions

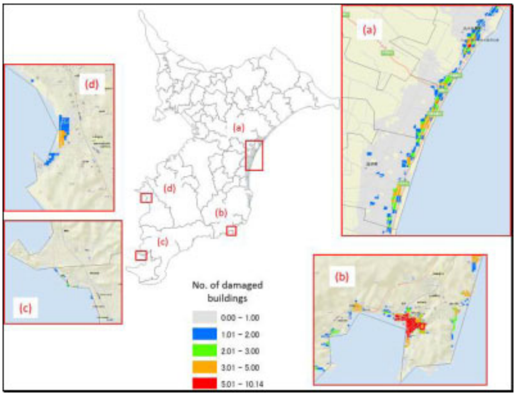

Figure 13. Estimated number of damaged buildings in Chiba Prefecture assuming the 1703 Genroku Kanto earthquake.

related to tsunami countermeasures in municipalities in which many buildings are predicted to be damaged severely.

5 CONCLUSIONS

This study evaluated the relationships between the damage ratio of buildings in Asahi City, Chiba Prefecture, and the hydrodynamic features of tsunami inundation flow estimated by numerical simulation after the 2011 off the Pacific coast of Tohoku (Tohoku-oki) earthquake. Tsunami inundation in Asahi City was numerically obtained using the leap-frog finite difference scheme. The tsunami heights were validated by comparing with field survey records.

Fragility functions for buildings were constructed with respect to inundation depth, current velocity, and hydrodynamic force. According to a comparison with those developed after previous events, the fragility function using the damage dataset compiled by Asahi City shows reasonable damage ratios if inundation depth is selected as the explanatory variable. Hence, the fragility function with respect to inundation depth was employed for damage assessment of buildings in Chiba Prefecture.

The 1677 Empo Boso-oki and 1703 Genroku Kanto earthquakes were used as scenario events for damage assessment. To estimate the number of damaged buildings, building inventory data compiled by Chiba Prefecture in 2008 and the results of numerical simulation of tsunami propagation were considered. The distributions of affected buildings along the Pacific coast of the prefecture were rather similar in both cases. Damage to buildings was observed along Tokyo Bay, western part of the prefecture, for the case of the 1703 Genroku Kanto earthquake. In total, more than 20,000 damaged buildings were predicted assuming the two historical events.

The results of this study may be helpful for making decisions related to tsunami countermeasures in municipalities in which severe damage to buildings is predicted. However, types of building structures could not be considered when constructing the fragility function of this study. Such effects should be investigated in a future study in order to perform a more detailed damage assessment of buildings.

REFERENCES

Asahi City, Chiba Prefecture. 2013. http://www.city.asahi.lg.jp/section/soumu/bousai_001.html (in Japanese).

Bertero, V.V., Corley, W.G., Degenkolb, H.J., Hakala, W.W., Hanson, R.D., Jirsa, J.O., Johnston, R.G., Krawinker, H., Lu, L., Mahin, S.A., McClamroch, N.H., Roeder, C.W., Sharpe, R., & Wight, J.K. 1985. Damage survey of the Nihon-Kai-Chubu, Japan Earthquake of May 26, 1983. *Earthquake Spectra* 1(2): 319–352.

Cabinet Office, Government of Japan. 2011. Outline of damage due to tsunami. http://www.bousai.go.jp/jishin/chubou/higashinihon/1/3-2.pdf (in Japanese).

EERI. 2011. The Tohoku, Japan Tsunami of March 11, 2011: Effects on Structures. EERI Special Earthquake Report—September 2011.

Fujii, Y., Satake, K., Sakai, S., Shinohara, M., & Kanazawa, T. 2011. Tsunami source of the 2011 off the Pacific coast of Tohoku Earthquake. *Earth Planets Space* 63: 815–820.

Furumura, T. & Saito, T. 2009. Integrated ground motion and tsunami simulation for the 1944 Tonankai earthquake using high-performance supercomputers. *Journal of Disaster Research* 4(2): 118–126.

Geospatial Information Authority of Japan. 2011. http://www.gsi.go.jp/cais/topic110422-index.html (in Japanese).

Imamura, F., 1995. Review of tsunami simulation with a finite difference method. *Long-Wave Runup Models*: 25–42. World Scientific.

Japanese National Police Agency. 2013. Damage situation and police countermeasures associated with 2011 Tohoku district – off the Pacific Ocean Earthquake. http://www.npa.go.jp/archive/keibi/biki/higaijokyo_e.pdf.

Kitamura, K., Maruyama, Y., & Yamazaki, F. 2012. Estimation of tsunami-inundated areas using satellite images and numerical model in Asahi city, Chiba Prefecture, after the 2011 off the Pacific coast of Tohoku earthquake. *Proceedings of the 33rd Asian Conference on Remote Sensing* Paper No. PS1-20, 10p.

Koshimura, S., Katada, T., Mofjeld, H.O., and Kawata, Y. 2006. A method for estimating casualties due to the tsunami inundation flow. *Natural Hazards* 39: 265–274.

Koshimura, S., Namegaya, Y., & Yanagisawa, H. 2009. Tsunami fragility – A new measure to identify tsunami damage. *Journal of Disaster Research* 4(6): 479–488.

Koshimura, S. & Kayaba, S. 2010. Tsunami fragility inferred from the 1993 Hokkaido Nansei-oki earthquake tsunami disaster. *Journal of Japan Association for Earthquake Engineering* 10(3): 87–101 (in Japanese).

Kotani, M., Imamura F., & Shuto, N. 1998. New method of tsunami runup and estimation of damage using GIS data. *Proceedings of the Coastal Engineering, Japan Society of Civil Engineers* 45: 356–360 (in Japanese).

Liu, P.L.F., Yeh, H. & Synolakis, C. 2008. Advanced numerical models for simulating tsunami wave and runup. *Advances in Coastal and Ocean Engineering* 10. World Scientific.

Ministry of Land, Infrastructure, Transport, and Tourism. 2011. http://www.mlit.go.jp/toshi/city_plan/crd_city_plan_tk_000005.html (in Japanese).

Namegaya, Y., Satake, K., & Shishikura, M. 2011. Fault models of the 1703 Genroku and 1923 Taisho Kanto earthquakes inferred from coastal movements in the southern Kanto area. *Annual Report on Active Fault and Paleoearthquake Researches* 11: 107–120 (in Japanese).

Ohmachi, T., Tsukiyama, H., & Matsumoto, H. 2001. Simulation of tsunami induced by dynamic displacement of seabed due to seismic faulting. *Bulletin of the Seismological Society of America* 91: 1898–1909.

Okada, Y. 1985. Surface deformation due to shear and tensile faults in a half-space. *Bulletin of the Seismological Society of America* 75(4): 1135-1154.

Ruangrassamee, A., Yanagisawa, H., Foytong, P., Lukkunaprasit, P., Koshimura, S., & Imamura, F. 2006. Investigation of tsunami-induced damage and fragility of buildings in Thailand after the December 2004 Indian Ocean Tsunami. *Earthquake Spectra* 22(S3): S377–S401.

Saatcioglu, M., Ghobarah, A., & Nistora, I. 2006. Performance of structures in Thailand during the December 2004 Great Sumatra Earthquake and Indian Ocean Tsunami. *Earthquake Spectra* 22(S3): S355–S375.

Shuto, N. 1991. Numerical simulation of tsunamis – Its present and near future. *Natural Hazards* 4: 171–191.

Shuto, N. 1993. Tsunami intensity and disasters. In S. Tinti (ed), *Tsunamis in the World*: 197–216. Kluwer Academic Publishers.

Stein, R.S., Toda, S., Parsons, T., & Grunewald, E. 2006. A new probabilistic seismic hazard assessment for greater Tokyo. *Philosophical Transactions of the Royal Society A* 364: 1965–1988.

Suppasri, A., Mas, E., Koshimura, S., Imai, K., Harada, K., & Imamura, F. 2012. Developing tsunami fragility curves from the surveyed data of the 2011 Great East Japan Tsunami in Sendai and Ishinomaki plains. *Coastal Engineering Journal* 54(1): Paper No. 1250008.

Takeuchi, H., Fuji, R., Mimura, N., Imamura, F., Satake, K., Tsuji, Y., Hochi, K., & Matsuura, T. 2007. Survey of run-up height of Empo Boso-oki Earthquake tsunami on the coast from Chiba Prefecture to Fukushima Prefecture. *Historical Earthquake* 22: 53–59 (in Japanese).

The 2011 Tohoku Earthquake Tsunami Joint Survey Group. 2011. Nationwide field survey of the 2011 off the Pacific Coast of Tohoku Earthquake tsunami. *Journal of Japan Society of Civil Engineers, Ser. B2* 67(1): 63–66.